

DOI: 10.1002/cbic.200800841

Analysis of Protein–Protein Interactions by Using Droplet-Based Microfluidics

Monpichar Srisa-Art,^[a] Dong-Ku Kang,^[b] Jongin Hong,^[a] Hyun Park,^[b] Robin J. Leatherbarrow,^[a] Joshua B. Edel,^[a, c] Soo-Ik Chang,^{*,[b]} and Andrew J. deMello^{*,[a]}

One of the primary goals of current proteomics research is to understand the physiological and metabolic pathways of cells and thereby establish molecular diagnostic tools that are able to identify the proteins associated with disease states. More specifically, protein–protein interactions are critical for many biological functions. For example, signal mediation between the exterior and interior of a cell is normally a result of protein–protein interactions. Such signal transduction plays an elementary role in many biological processes and in many diseases (such as cancer). Accordingly, the ability to probe protein–protein interactions in a high-throughput manner is recognised to be important in developing effective diagnostic techniques, cultivating disease therapies and discovering new small-molecule drug candidates.

To date, two-dimensional gel electrophoresis and mass spectroscopy have been the workhorses of proteomics research. However, the difficulties associated with the analysis and quantitation of low-abundance, high-molecular-weight and hydrophobic proteins expressed in cells have hindered attempts at high-throughput protein analysis. Over the past decade protein-microarray technology has been developed to address these limitations. Protein microarrays allow the simultaneous analysis of thousands of different binding events including DNA–protein,^[1] protein–protein,^[2] receptor–ligand,^[3,4] enzyme–substrate^[5–7] and protein–drug^[8] interactions within a single experiment, and additionally facilitate the evaluation of a large number of biochemical structures against hundreds of biological targets. The main advantage of array-based technologies over conventional analysis methods is the ability to perform massively parallel analyses with reduced sample and reagent volumes. Nevertheless, in array-based systems, capture proteins must be immobilized onto a surface. This can lead to a heterogeneity in the immobilized protein activity. Additionally,

protein-immobilization strategies might not be perfectly suited to probing protein–protein interactions under physiological conditions, since obstruction or deformation of the protein binding sites through interaction with a solid surface can significantly interfere with specific protein–protein interactions. Furthermore, extended incubation times, repetition of washing stages and the involvement of blocking proteins have been shown to compromise the activities of target proteins, the accurate determination of protein–protein interactions and analysis times.

Recently, the manipulation of multiphase flows in microfluidic systems has been introduced as a fundamental experimental platform for high-throughput experimentation.^[9–13] These systems enable the generation and manipulation of monodisperse bubbles or liquid droplets in an immiscible carrier fluid. Such encapsulated droplets can be used to mimic artificial cells or isolated reaction vessels. Indeed, droplet-based microfluidic systems have been applied to a range of chemical and biological problems including enzymatic assays,^[9] protein crystallization,^[9] nanomaterial synthesis,^[10–13] high-throughput binding assays,^[14] real-time binding kinetics^[15] and cell-based assays.^[16,17] Compared to conventional, single-phase microfluidic systems, the localization of reagents within discrete and isolated droplets has been shown to be an extremely effective way of enhancing the reaction yields for diffusion-limited reactions and eliminating residence time distributions.^[9,13] Moreover, the ability to generate controllably droplets with changeable reagent composition and at rates in excess of 1 kHz means, in theory, that millions of individual reactions or assays can be processed in very short times. However, before this system can become a core instrumental platform in chemistry and biology, the significant challenge of on-line droplet detection with high sensitivity and speed must be overcome. In this communication, we apply FRET measurements in a segmented-flow microfluidic platform to the analysis of protein–protein interactions.

Angiogenin (ANG), a small polypeptide implicated in angiogenesis and in tumour growth, has a unique ribonucleolytic activity and undergoes nuclear translocation in proliferating endothelial cells.^[18,19] It was selected as a model protein to confirm the efficacy of our experimental approach. Specifically, an anti-ANG antibody (anti-ANG Ab) and an ANG antigen were labelled with fluorophores to act as donor and acceptor, respectively, in the FRET measurements. The acceptor (Alexa Fluor 647; AF647) was linked with the donor (Alexa Fluor 488; AF488) by antigen–antibody binding (Figure 1A). FRET can occur since the fluorescence emission spectrum of AF488 overlaps with the absorption spectrum of AF647. Figure 1B shows fluorescence emission spectra of a mixture of anti-ANG Ab-

[a] M. Srisa-Art,[†] Dr. J. Hong,[†] Prof. R. J. Leatherbarrow, Dr. J. B. Edel, Prof. A. J. deMello
Department of Chemistry, Imperial College London
Exhibition Road, London SW7 2AZ (UK)
Fax: (+44)207-594-5801
E-mail: a.demello@imperial.ac.uk

[b] Dr. D.-K. Kang,[†] H. Park, Prof. S.-I. Chang
Department of Biochemistry
Protein Chip Research Centre Chungbuk National University
Cheongju, Chungbuk 361–763 (Korea)
Fax: (+82)43-267-2306
E-mail: sichang@cbnu.ac.kr

[c] Dr. J. B. Edel
Institute of Biomedical Engineering, Imperial College London
South Kensington Campus, London SW7 2AZ (UK)
Fax: (+44)207-594-5196

[†] These authors contributed equally to this work.

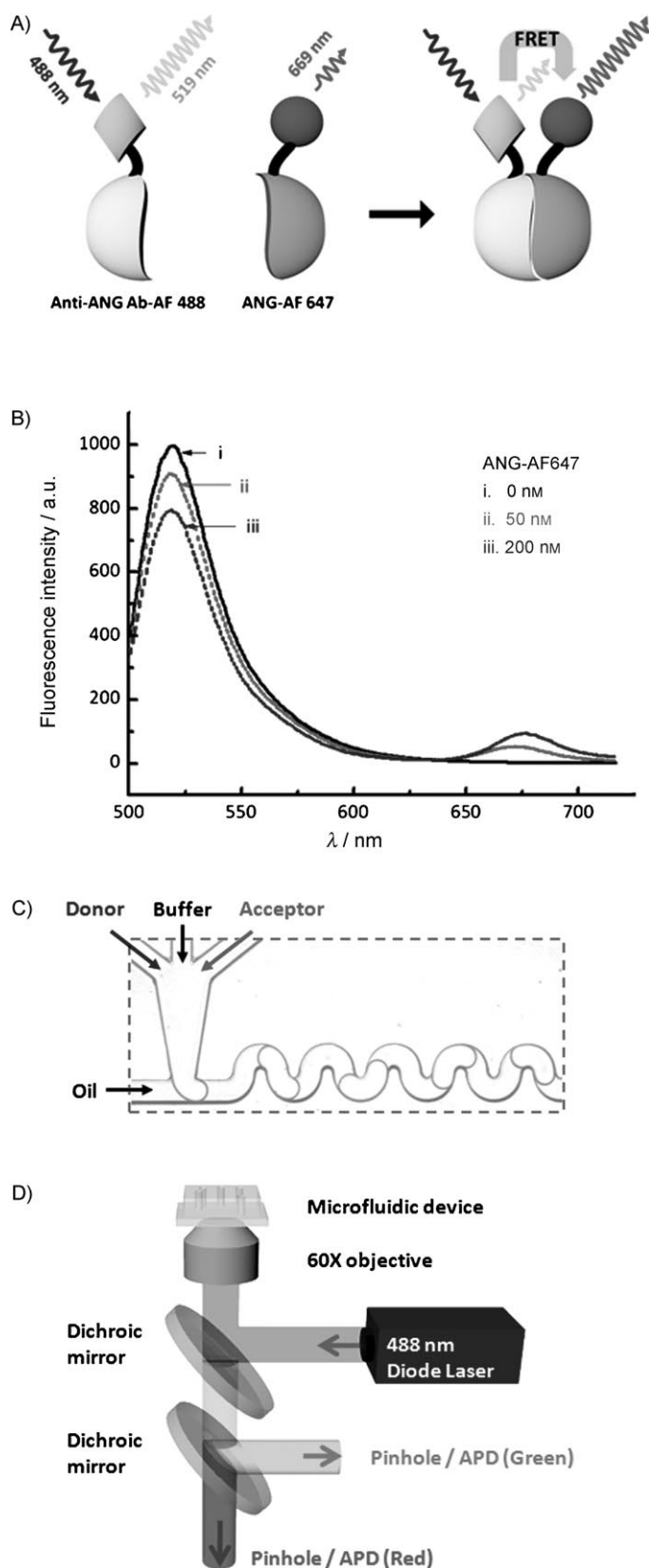


Figure 1. A) Schematic of FRET facilitated by protein–protein binding. B) Fluorescence emission spectra of a mixture of anti-ANG Ab-AF488 and ANG-AF647. The anti-ANG Ab-AF488 concentration was fixed at 10 nM, whilst the ANG-AF647 concentration was varied (0, 50 and 200 nM). C) Image of droplets generated within the microfluidic device. D) A schematic of the optical setup used for fluorescence measurements.

AF488 and ANG-AF647. The peak at 519 nm corresponds to AF488 emission, with the peak at 669 nm corresponding to emission from AF647. As the concentration of ANG-AF647 increases, the intensity at 519 nm decreases whilst that at 669 nm increases.

Droplet-based binding experiments were performed by using a polydimethylsiloxane (PDMS) microfluidic device containing three aqueous inlets, one oil inlet and a single outlet. A schematic of the microfluidic device is shown in Figure 1C. Here, anti-ANG Ab-AF488 is delivered through the left inlet, while ANG-AF647 is delivered through the right inlet. A central buffer stream is introduced through the middle inlet to prevent mixing of the sample streams prior to droplet formation. This arrangement ensures that binding and subsequent FRET occur only after the sample has been encapsulated inside a droplet. Droplets have an average volume of approximately 350 pL and were generated at 20 Hz. A two-colour fluorescence-detection system was used to simultaneously record green and red fluorescence emission from the donor (AF488) and the acceptor (AF647) moieties, respectively (Figure 1D).

Typical FRET fluorescence burst scans over a time interval of 1 s are presented in Figure 2. Significantly, green (light grey trace) and red (dark grey trace) signals, corresponding to AF488 and AF647 emission, respectively, are coincident due to FRET. Inspection of Figure 2 demonstrates that the red signal increases as a function of ANG-AF647 concentration; this indicates that more ANG molecules are binding to the anti-ANG Ab. Conversely, the green droplet signature essentially decreases because of energy transfer. Nevertheless, it must also be realised that the red fluorescence signal is a convolution of fluorescence from FRET and a background contribution due to direct excitation of the acceptor fluorophore by the excitation source and detector crosstalk (leakage of donor emission into the acceptor or red detector). We have previously established that crosstalk for this particular FRET pair is only 1.2%,^[14] and is thus negligible. Accordingly, for precise determination of fluorescence intensities, photon counts from the acceptor detector were corrected by using the following relationship [Eq. (1)]:

$$I'_A = I_A - \left(I_{Ag} \times \frac{C'_A}{C_{Ag}} \right) \quad (1)$$

Here I_A and I'_A are photon counts from the energy acceptor (red) detector before and after correction. I_{Ag} represents the photon counts measured by the energy-acceptor detector when analysing only ANG-AF647 at a concentration of C_{Ag} , and C'_A defines the concentration of ANG-AF647 in each experiment. FRET efficiency (E_{FRET}) is given by ref. [14] [Eq. (2)]:

$$E_{\text{FRET}} = \frac{I'_A}{I'_A + I_D} \quad (2)$$

Here I_D defines photon counts originating from the energy donor (green) detector. E_{FRET} is plotted as a function of the concentration of ANG-AF647 in Figure 3A. The E_{FRET} value reflects binding of ANG to the anti-ANG Ab and follows a saturation binding model^[20] [Eq. (3)]:

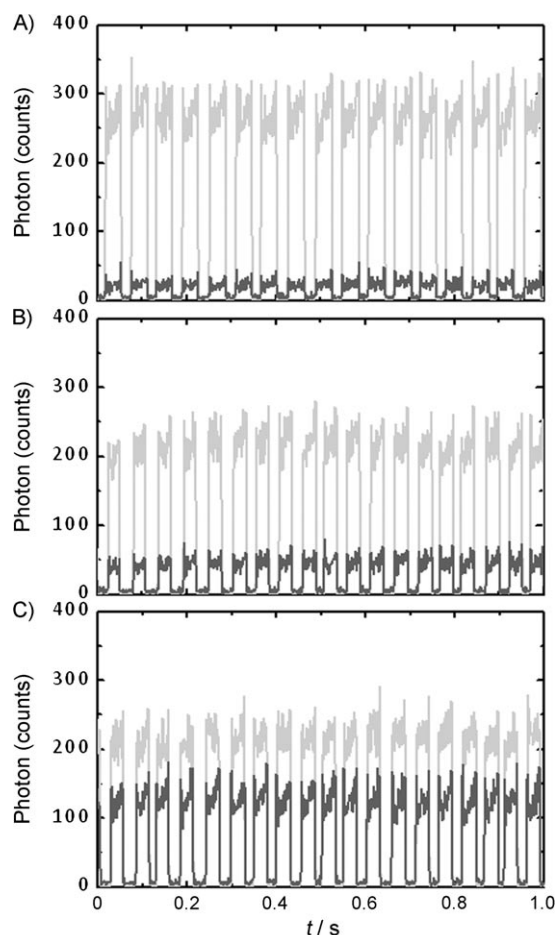


Figure 2. Example fluorescence burst scans recorded over a time period of 1 s with a 50 ns bin time. The concentration of the anti-angiogenin antibody labelled with Alexa Fluor 488 (anti-ANG Ab-AF488; light grey trace) was fixed at 10 nM, while the concentration of angiogenin labelled with Alexa Fluor 647 (ANG-AF647; dark grey trace) was varied from A) 0.6 nM to B) 3.0 nM to C) 6.6 nM.

$$E_{\text{FRET}} = (E_{\text{FRET}})_{\text{max}} \cdot \frac{[A]}{K_D + [A]} \quad (3)$$

Here K_D is the dissociation constant, and $[A]$ is the concentration of the ANG-AF647 that remains unbound. If the concentration of antibody, $[Ab]_0$, is low relative to $[A]$, then the total concentration of A can be taken to be the same as the unbound concentration, and the data in Figure 3A can be fitted directly to the above model. A nonlinear least-squares fit of the data yields $K_D = 16.6 \pm 2.5$ nM and $(E_{\text{FRET}})_{\text{max}} = 1.20 \pm 0.07$.

High-affinity interactions often display the complication of tight binding kinetics, which occurs when the total concentration of the binding partner cannot be assumed to be equal to the unbound concentration. In this case, inspection of Figure 3A shows that, at $[A] = 10$ nM, close to 50% of the material is bound. In these experiments, the initial concentration of antibody was 10 nM, and therefore it is necessary to take into account the concentration of antibody, $[Ab]_0$, by using the tight-binding Equation (4), that is:

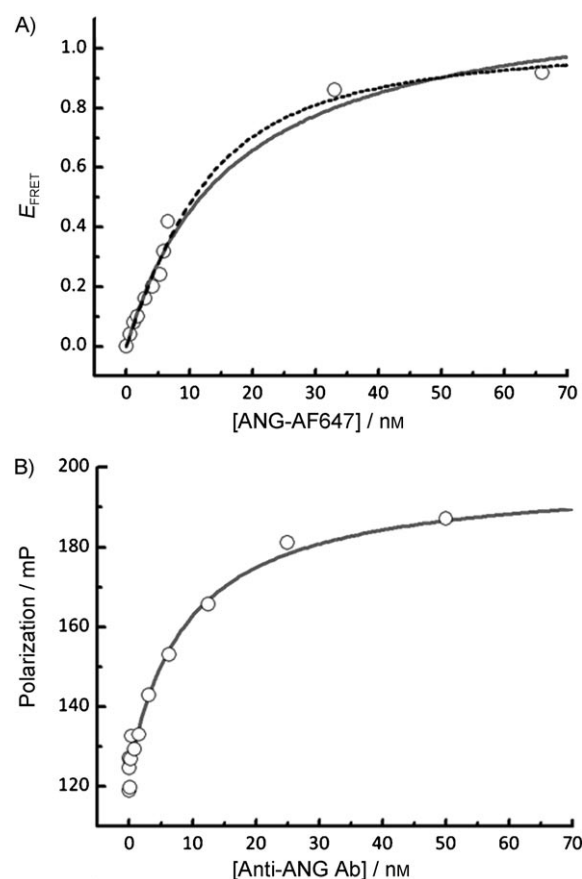


Figure 3. Binding of angiogenin (ANG) with anti-angiogenin antibody (anti-ANG Ab) by A) droplet-based microfluidic experiments and B) bulk fluorescence polarization measurements (grey line: non-tight binding fit, black dotted line: tight binding).

$$E_{\text{FRET}} = (E_{\text{FRET}})_{\text{max}} \left[1 - \frac{([Ab]_0 + [A] + K_D) - \sqrt{([Ab]_0 + [A] + K_D)^2 - 4[Ab]_0[A]}}{2[Ab]_0} \right] \quad (4)$$

A nonlinear least-squares fit to this equation, for $[Ab]_0 = 10$ nM, yields $K_D = 6.4 \pm 1.6$ nM and $(E_{\text{FRET}})_{\text{max}} = 1.04 \pm 0.05$. Under the conditions used, the data are well modelled by the tight-binding equation. Moreover, this model also gives an $(E_{\text{FRET}})_{\text{max}}$ value that is close to the expected maximum of 1.0.

The results from the droplet-based microfluidic device were compared to values obtained by using more conventional measurements performed in solution. Bulk fluorescence polarization (FP) measurements were performed on a Beacon 2000 polarization spectrometer (Panvera, Madison, WI, USA). Figure 3B illustrates the binding of fluorescein-labelled angiogenin (ANG-FITC) with anti-ANG Ab by fluorescence polarization (mP) plotted as a function of the total concentration of anti-ANG Ab. Data were modelled by using Equation (5):^[21]

$$P = P_{\text{min}} + \Delta P \frac{[\text{anti-ANG Ab}]}{K_D + [\text{anti-ANG Ab}]} \quad (5)$$

Here P , ΔP and $[\text{anti-ANG Ab}]$ are the measured polarization, the total change in polarization and the total concentration of

anti-ANG Ab, respectively. A nonlinear least-squares fit of the data yields $K_D = 9.0 \pm 1.5$ nM, $P_{\min} = 123.6 \pm 1.3$ mP and $\Delta P = 74.4 \pm 3.3$ mP. These experiments utilized 1.3 nM ANG-FITC, which is low enough not to deplete the concentration of anti-ANG Ab significantly. Importantly, it can be seen that the K_D values extracted from the droplet-based binding experiments are comparable with data generated from the bulk-fluorescence polarization measurements, thus confirming that droplet-based measurements reach equilibrium prior to the acquisition of fluorescence data.

The obtained data points in Figure 3B were also fitted to a Hill equation so as to assess the existence of multiple binding sites^[21] [Eq. (6)]:

$$P = P_{\min} + \Delta P \frac{[\text{anti-ANG Ab}]^n}{(K_D)^n + [\text{anti-ANG Ab}]^n} \quad (6)$$

A Hill coefficient (n) of 1.0 indicates a single binding site and a value significantly different from 1.0 indicates either cooperativity or multiple binding modes. The nonlinear least-squares fit yields $K_D = 8.7 \pm 2.0$ nM, $P_{\min} = 123.9 \pm 1.6$ mP, $\Delta P = 73.0 \pm 6.7$ mP and $n = 1.04 \pm 0.18$, thus showing that the data are consistent with a single class of binding site.

AF488 labelling sites in the anti-ANG Ab were determined by pepsinolysis or disulfide bond cleavage of the anti-ANG Ab-AF488. Pepsin was used to digest the Fc portion of whole IgG to yield $F(ab')_2$ fragments.^[20] Figure 4B and C shows SDS-PAGE images of anti-ANG Ab-AF488 after incubation with a reducing agent (2-mercaptoethanol) or after digestion with pepsin. The results suggest that the AF488 labelling sites in the anti-ANG Ab are in the heavy chain of $F(ab')_2$ fragments. The protein-to-dye ratios for ANG-AF647, anti-ANG Ab-AF488 and ANG-FITC were also calculated to be 0.35, 2.0 and 0.28, respectively.

The effects of modification of either ANG or anti-ANG Ab by the fluorescent labels on the biological and enzymatic activities were examined by nuclear translocation, ribonucleolytic and Western blot assays. Nuclear translocation of the ANG-AF647 in human umbilical vein endothelial (HUVE) cells was observed to be the same as in the native ANG (Figure 5A). Activity toward poly(C) was determined by measuring the rate of formation of perchloric acid-soluble products.^[22] It was observed that the ribonucleolytic activity of ANG-AF647 is also comparable to that of native ANG (Figure 5B). Both the native ANG and ANG-AF647 were specifically recognised by either anti-ANG Ab-AF488 or native anti-ANG Ab, and the activity of equal amounts of ANG-AF647 and native ANG toward anti-ANG Ab-AF488 or the native anti-ANG Ab is essentially the same (Figure 5C). These results indicate that the modification of ANG by the fluorophore AF647 does not alter its biological or enzymatic activity and that the modification of anti-ANG Ab by the fluorophore AF488 does not alter its binding activity or its recognition of ANG.

In summary, we have successfully demonstrated FRET-based analysis of protein-protein interactions in thousands of picolitre-sized droplets. Extracted K_D values of ANG and anti-ANG Ab from the droplet-based microfluidic experiments ($K_D = 6.4 \pm 1.6$ nM) are shown to agree closely with data obtained from

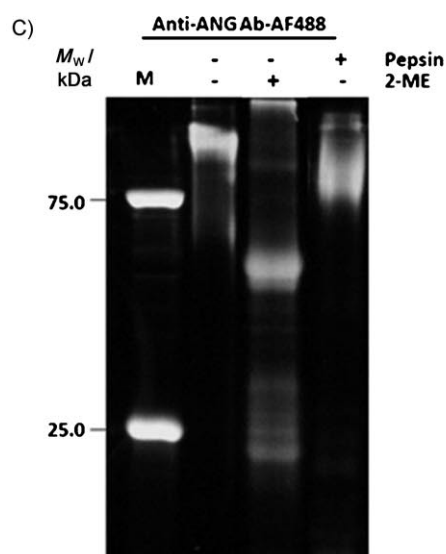
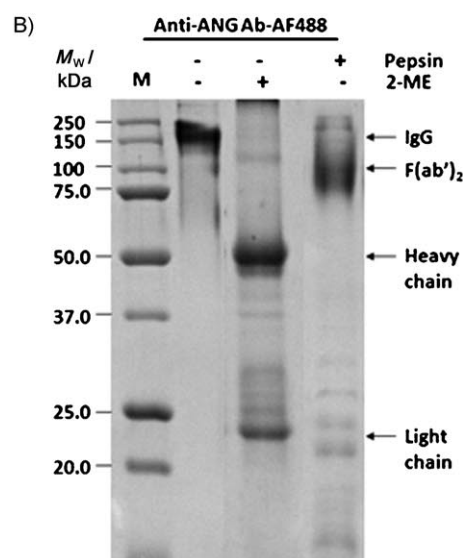
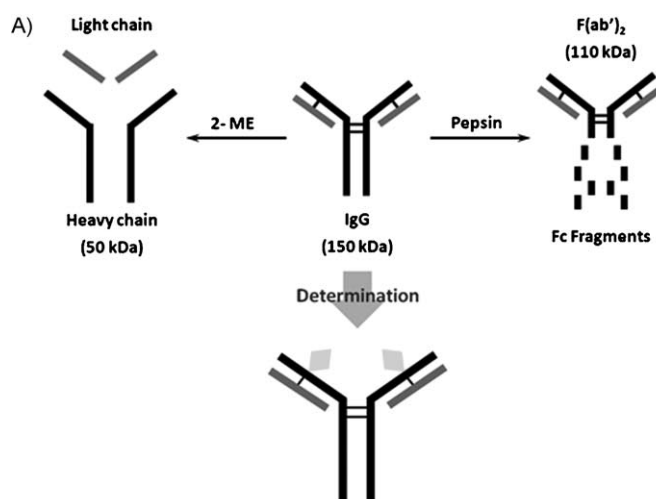


Figure 4. A) Reduction and digestion scheme for preparing $F(ab')_2$ and heavy/light chain fragments from IgG antibodies. B) Coomassie staining and C) fluorescence detection of SDS-PAGE of anti-ANG Ab-AF488 after incubation with 2.9 mM 2-mercaptoethanol (2-ME) or after digestion with pepsin.

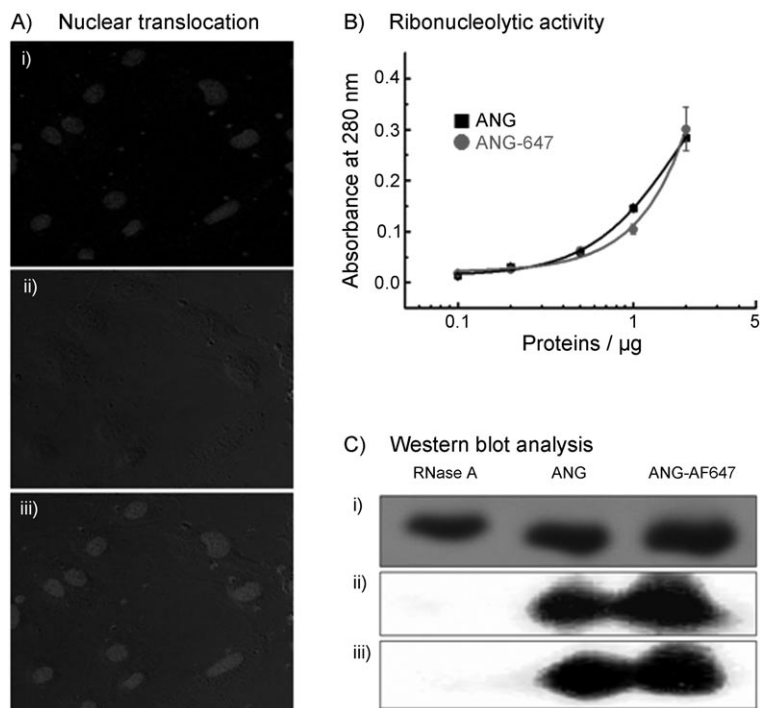


Figure 5. A) Nuclear translocation of ANG-AF647. i) fluorescein fluorescence, ii) transmission and iii) merged images. B) Ribonucleolytic activities of ANG (■) and ANG-AF647 (●). C) i: SDS-PAGE of RNase A, ANG and ANG-AF647 and their Western blot analysis by ii: anti-ANG Ab and iii: anti-ANG Ab-AF488.

bulk-fluorescence polarization measurements ($K_D = 9.0 \pm 1.5$ nM). Importantly, the use of AF488 and AF647 as acceptor and donor in FRET analysis, does not affect the biological and enzymatic activity of ANG or the binding activities of anti-ANG Ab to ANG. This validates the use of labelled ANG and anti-ANG Ab for monitoring protein–protein interactions in droplet-based microfluidic systems. We expect that such an experimental platform will have significant applicability in the high-throughput analysis of protein–protein interactions. Indeed in vitro compartmentalization within aqueous microdroplets combined with high-sensitivity fluorescence detection has the capacity to allow the rapid and facile probing of interactions between large chemical/peptide libraries and potential targets under a variety of experimental conditions. Current studies are exploring the application of this platform technology to the screening of angiogenin inhibitors, which inhibit interactions between angiogenin and anti-angiogenin antibodies, together with large combinatorial peptide libraries.^[23]

Experimental Section

Expression and purification of angiogenin (ANG): *E. coli* strain Rosetta (DE3)pLysS, carrying the ANG gene, was used for expression of angiogenin.^[24] Isolated inclusion bodies were dissolved in guanidine hydrochloride (GdnHCl; 6 M), Tris/HCl (100 mM, pH 8), EDTA (1 mM), NaCl (100 mM) and reduced DTT (DTTred; 10 mM). Solutions of inclusion bodies were diluted for refolding to 0.2 mg protein per mL in a Tris/HCl buffer (100 mM, pH 8) containing DTTred (0.5 mM), GdnHCl (0.3 M), EDTA (1 mM), GSSG (0.3 mM) and GSH

(1.5 mM), and were then incubated for 24 h at 4 °C. Once folding was judged to be complete, the solution was concentrated by ultrafiltration and then loaded onto a cation-exchange FPLC column packed with SP-sepharose Fast Flow (GE Healthcare Life Sciences, USA) and equilibrated with Tris/HCl (25 mM, pH 8). The collected fractions from the FPLC column were dialysed against water and lyophilised. The purified ANG was characterized by various analytical methods, including N-terminal sequencing, mass spectrometry, circular dichroism and bioassays.

Production and purification of anti-angiogenin antibody (anti-ANG Ab): The anti-ANG Ab was purified from rabbit serum by injecting the rabbit with ANG and waiting for an immune reaction, as previously described.^[25]

Fluorescence labelling: The purified ANG and anti-ANG Ab were labelled with Alexa Fluor 647 (AF647) and Alexa Fluor 488 (AF488), respectively, by using an Alexa Fluor 488/647 protein-labelling kit (Invitrogen) according to the manufacturer's protocol. The Alexa Fluor-conjugated proteins were purified by using a Sephadex™ G-25 column (GE Healthcare). For FP experiments, ANG was labelled with fluorescein by using a Fluorotag™ FITC conjugation kit (Sigma). Protein solutions were assessed for labelling efficiency by using predetermined extinction coefficients for the fluorophores at their respective absorbance maxima and 280 nm, as described in the technical bulletin (Invitrogen, Sigma).

Pepsinolysis: The anti-ANG Ab-AF488 (5 μg) was incubated with pepsin (4 μL of 1 mg mL⁻¹) in sodium acetate buffer (0.1 M, pH 4.0) for 6 h at 37 °C. The reaction was terminated by adding nondenaturing condition sample buffer (Tris-HCl (63 mM), glycerol (10%) and Bromophenol blue (0.01%), pH 6.8). F-(ab')₂ fragments from IgG after pepsinolysis were size-separated by electrophoresis on SDS-poly acrylamide gels (12%) and stained with Coomassie Blue. The locations of AF488 in IgG were also visualized by fluorescence.

Nuclear translocation of ANG-AF647 in HUVE cells: Human umbilical vein endothelial (HUVE) cells were trypsinized, seeded at 5×10^3 cells per cm² on a 18 × 18 mm cover glass placed in six-well culture plates, and cultured in EGM-2 (Lonza, Basel, Switzerland) for 24 h. After being washed with prewarmed PBS, HUVE cells were cultured in EBM-2 (Lonza) supplemented with fetal bovine serum (FBS; 1%) for 12 h. The cells were washed three times with prewarmed (37 °C) EBM-2 (Lonza) supplemented with FBS (1%). A washed cover glass was mounted in a modified chamber positioned on the platform of an inverted-laser confocal microscope (TCS SP2 AOBS, Leica). To incubate cells in prewarmed (37 °C) EBM-2 with AF647 (1 μg mL⁻¹) conjugated angiogenin (ANG-AF647), exchange of the 0.5 mL chamber volume was achieved with manual volume replacement by pipetting from the above. After 30 min, the chamber was washed with prewarmed (37 °C) EBM-2, and then fluorescence was observed with a confocal-laser scanning microscope (TCS SP2 AOBS).

Enzymatic assay: The ribonucleolytic activities of the native ANG and ANG-AF647 were determined by measuring the rate of formation of perchloric acid-soluble products in poly(C) precipitation assay.^[23] Briefly, serial dilutions of ANG or ANG-AF647 were incubated with poly(C) (60 μL of 2 mg mL⁻¹) in HEPES (30 mM, pH 7) for 4 h at 37 °C. The reaction was terminated by chilling the mixture on ice and adding cold perchloric acid (3.4%, 700 μL). After 10 min

on ice, the samples were separated in a centrifuge at 22000g for 10 min at 4 °C. The supernatant of each sample was measured at an absorbance of 280 nm. All readings were corrected for the absorbance of blanks that lacked ANG or ANG-AF647. The assays were carried out in duplicate.

Western blot analysis: The native ANG and ANG-AF647 were size-separated by electrophoresis on SDS-poly acrylamide gels (15%) and transferred electrophoretically to a poly(vinylidene difluoride) membrane. Nonspecific binding was blocked by PBS containing skimmed milk (5%) for 3 h at 25 °C. The membrane was immunoblotted with the native anti-ANG Ab or anti-ANG Ab-AF488 for 12 h at 4 °C and then exposed to a horseradish peroxidase-conjugated secondary antibody (1:2000 dilution in PBS) for 1 h at 25 °C. Immunoreactive spots were visualized by using an enhanced chemiluminescence (ECL) detection system.

Droplet-based binding experiments: A polydimethylsiloxane (PDMS) microfluidic device with three aqueous inlets was used in the protein FRET experiments that conceptual antigen–antibody interactions are superimposed on. The completed microfluidic device was placed onto a controllable stage (ProScan II™, Prior Scientific Instruments Ltd., Cambridge, UK) of the microscope. Precision syringe pumps (PHD 2000, Harvard Apparatus, Edenbridge, UK) were used to deliver reagent solutions at flow rates ranging from 0.1 to 1.5 $\mu\text{L min}^{-1}$ using gas-tight syringes (2.5 mL for oil and 1 mL for aqueous solutions; SGE Analytical Science, SGE Europe Ltd., Milton Keynes, UK). Perfluorodecalin/1H,1H,2H,2H-perfluorooctanol (10:1, v/v) was used as the continuous oil phase for all experiments. All liquids were filtered by using 0.2 μm syringe filters (Pall Corporation, East Hills, USA) before use. Two protein solutions and PBS buffer were introduced separately through the three aqueous inlets. Accordingly, on-line dilution can be performed by changing the relative flow rates of three aqueous streams (from 0.1 to 1.1 $\mu\text{L min}^{-1}$), but keeping the total aqueous flow rate constant to maintain the droplet size. Fluorescence measurement of droplets was carried out by using a custom-built confocal laser integrated with an Olympus IX71 microscope. This confocal setup consists of a 488 nm diode laser, as an excitation source, and a dual detection system. The laser beam was aligned into the microscope body by using beam-steering optic mirrors. The beam was then reflected by a dichroic mirror (z488rdc, Chroma Technology Corp., Rockingham, USA) into a 60 \times water immersion objective (Olympus) and then tightly focused onto the microfluidic channel. The fluorescence was collected by the same objective, spectrally filtered from the excitation light by using an emission filter (z488Lp, Chroma Technology Corp.), and then passed through a 75 μm pinhole (Thorlabs, Ely, UK). The fluorescence signal was further separated by another dichroic mirror (630dcxr, Chroma Technology Corp.) to be detected simultaneously by two avalanche photodiode detectors (AQR-141, EG&G, Perkin–Elmer). The reflected light (green fluorescence), filtered by an hq540/80 m emission filter (Chroma Technology Corp.), was detected by the first (donor) detector. The transmitted light (red fluorescence), filtered by an hq640Lp emission filter (Chroma Technology Corp.), was detected by the second (acceptor) detector. Data were collected from the detectors by using a multifunction DAQ device for data logging (PCI 6602, National Instruments, Newbury, UK), which was controlled by using a programme written in LabView (National Instruments). Data were collected over a period of 60 s (or 1200 droplets). Binding data were generated by using measurements from a series of reactions in which the concentration of the ANG-AF647 was varied, whilst keeping the anti-ANG Ab-AF488 concentration constant at 10 nM.

Values of K_D were determined through analysis of the binding data using GraFit (Erithacus Software Ltd., Horley, UK).

Bulk spectroscopic measurements: Fluorescence-emission spectrum measurements were performed on a Luminescence Spectrometer (Perkin–Elmer). Anti-ANG Ab-AF488 (10 nM) was titrated with ANG-AF647 (1–200 nM), and the fluorescence emission (excitation at 488 nm) was monitored. Fluorescence-polarization measurements were performed on a Beacon 2000 polarization spectrometer (Panvera, USA). Fluorescein-labelled angiogenin (ANG-FITC, 1.3 nM) was titrated with anti-ANG Ab (0.01–100 nM), and the fluorescence polarization was monitored. Values of K_D were determined through analysis of data by using GraFit (Erithacus Software).

Acknowledgements

M.S.-A. would like to acknowledge the Royal Thai Government for financial support. This work was partially supported by the RCUK-funded Microdroplets Basic Technology Project, the DIUS- and KICOS- (K20602000681-08B0100-02210) funded UK/Korea Focal Point Programme on Life Science, the Korea Science and Engineering Foundation (M10749000231-08N4900-23110) and the Korea Biotech R&D Group of Next-Generation Growth Engine Project (F104AB010004-08A0201-00410).

Keywords: angiogenin antibody · angiogenin · microdroplets · microfluidics · protein–protein interactions

- [1] M. L. Bulyk, E. Gentalen, D. J. Lockhart, G. M. Church, *Nat. Biotechnol.* **1999**, *17*, 573.
- [2] G. MacBeath, *J. Am. Chem. Soc.* **1999**, *121*, 7967.
- [3] U. B. Nielsen, M. H. Cardone, A. J. Sinskey, G. MacBeath, P. K. Sorger, *Proc. Natl. Acad. Sci. USA* **2003**, *100*, 9330.
- [4] P. Arenkov, A. Kukhtin, A. Gemell, S. Voloshchuk, V. Chupeeva, A. Mirzabekov, *Anal. Biochem.* **2000**, *278*, 123.
- [5] H. Zhu, J. F. Klemic, S. Chang, P. Bertone, A. Casamayor, K. G. Klemic, D. Smith, M. Gerstein, M. A. Reed, M. Snyder, *Nat. Genet.* **2000**, *26*, 283.
- [6] H. Zhu, M. Bilgin, R. Bangham, D. Hall, A. Casamayor, P. Bertone, N. Lan, R. Jansen, S. Bidlingmaier, T. Houfek, T. Mitchell, P. Miller, R. A. Dean, M. Gerstein, M. Snyder, *Science* **2001**, *293*, 2101.
- [7] J. Ziauddin, D. M. Sabatini, *Nature* **2001**, *411*, 107.
- [8] M. F. Templin, D. Stoll, M. Schrenk, P. C. Traub, C. F. Vohringer, T. O. Joos, *Trends Biotechnol.* **2002**, *20*, 160.
- [9] H. Song, D. L. Chen, R. F. Ismagilov, *Angew. Chem.* **2006**, *118*, 7494; *Angew. Chem. Int. Ed.* **2006**, *45*, 7336.
- [10] A. J. deMello, *Nature* **2006**, *442*, 394.
- [11] A. Gunther, K. F. Jensen, *Lab Chip* **2006**, *6*, 1487.
- [12] S. Y. Teh, R. Lin, L. H. Hung, A. P. Lee, *Lab Chip* **2008**, *8*, 198.
- [13] A. Huebner, S. Sharma, M. Srisa-Art, F. Hollfelder, J. B. Edel, A. J. deMello, *Lab Chip* **2008**, *8*, 1244.
- [14] M. Srisa-Art, A. J. deMello, J. B. Edel, *Anal. Chem.* **2007**, *79*, 6682.
- [15] M. Srisa-Art, E. C. Dyson, A. J. deMello, J. B. Edel, *Anal. Chem.* **2008**, *80*, 7063.
- [16] M. Y. He, J. S. Edgar, G. D. M. Jeffries, R. M. Lerez, J. P. Shelby, D. T. Chiu, *Anal. Chem.* **2005**, *77*, 1539.
- [17] A. Huebner, M. Srisa-Art, D. Holt, C. Abell, F. Hollfelder, A. J. deMello, J. B. Edel, *Chem. Commun.* **2007**, 1218.
- [18] J. W. Fett, D. J. Strydom, R. R. Lobb, E. M. Alderman, J. L. Bethune, F. Riordan, B. L. Vallee, *Biochemistry* **1985**, *24*, 5480.
- [19] N. Yoshioka, L. Wang, K. Kishimoto, T. Tsuji, G. F. Hu, *Proc. Natl. Acad. Sci. USA* **2006**, *103*, 14519.
- [20] A. Moro, T. Yoshitake, T. Ogawa, T. Ichimura, *J. Biochem.* **2008**, *144*, 733.
- [21] J. A. Goodrich, J. F. Kugel, *Binding and Kinetics for Molecular Biologists*, Cold Spring Harbor Laboratory Press, New York, **2007**.

- [22] N. Russo, V. Nobile, A. D. Donato, J. R. Riordan, B. L. Vallee, *Proc. Natl. Acad. Sci. USA* **1996**, *93*, 3243.
- [23] R. A. Houghten, P. Clemencia, J. R. Appel, S. E. Blondelle, C. T. Dooley, J. Eichler, A. Nefzi, J. M. Ostresh, *J. Med. Chem.* **1999**, *42*, 3743.
- [24] S.-H. Jang, D.-K. Kang, S.-I. Chang, H. A. Scheraga, H.-C. Shin, *Biotechnol. Lett.* **2004**, *26*, 1501.
- [25] S.-I. Chang, G.-G. Jeong, S.-H. Park, B.-C. Ahn, J.-D. Choi, Q. Chae, S. K. Namgoong, S.-I. Chung, *Biochem. Biophys. Res. Commun.* **1997**, *232*, 323.

Received: December 22, 2008

Please note: Minor changes have been made to this manuscript since its publication in *ChemBioChem* Early View. The Editor.

Published online on June 3, 2009
